

Inkjet Printed Highly Transparent and Flexible Graphene Micro-Supercapacitors

Szymon Sollami Delekta, Anderson D. Smith, Jiantong Li, Mikael Östling*

S. Sollami Delekta, Dr. A. D. Smith, Dr. J. Li, Prof. M. Östling

KTH Royal Institute of Technology

School of Information and Communication Technology

Electrum 229, SE-164 40 Kista, Sweden

E-mail: jiantong@kth.se

Supporting information

Materials and methods

Formulation of graphene inks

The graphene inks, consisting of ~0.5 mg/mL graphene nanosheets, 2 mg/mL ethyl cellulose (viscosity 4 cP for 5 w/v% in 80:20 toluene:ethanol, Sigma-Aldrich, product number: 200646) and 8 mg/mL ethyl cellulose (viscosity 22 cP for 5 w/v% in 80:20 toluene:ethanol, Sigma-Aldrich, product number: 200697) in terpineol, were formulated through the ultrasonication-assisted exfoliation of graphite (Sigma-Aldrich, product number: 332461) followed by the solvent exchange technique as previously reported.^{1,2} Then, the graphene inks were diluted with ethanol at the volume ratio of 3:1 (terpineol:ethanol).

Printing

All the devices were printed using a commercial piezoelectric inkjet printer (Dimatix Materials Printer, DMP 2800, Dimatix-Fujifilm Inc.) and 10 pL cartridges (DMC-11610). The graphene flakes were printed with a drop spacing of 40 μm , jetting voltage of 27 V and plate temperature between 30 °C and 45 °C. For the hard mask, silver ink (Cabot Conductive Ink CCI-300, Cabot Corporation) was printed with a drop spacing of 30 μm , jetting voltage of 26 V and plate temperature of 45 °C.

Device Fabrication

The graphene inks were printed on untreated microscope glass slides (SuperFrost Slides, VWR, product number: 631-0114) or flexible glass (Corning Willow glass, 100 μm thick, Corning). The films were then dried at 80 °C for 1 to 2 hours.

Since the graphene inks consist of a high boiling point solvent (terpineol) and a low boiling point solvent (ethanol), at this temperature the ethanol rapidly evaporates and the remaining terpineol forms a very viscous film which efficiently prevents local flows of solute. Once dry, the films were annealed at 400 °C for 1 hour. Then, the hard mask was printed with silver ink and dried at 80 °C for 1 hour. Next, the exposed graphene flakes were etched with O₂ plasma (Plasmalab80Plus, Oxford RIE System, Oxford Plasma Technology) for 20 min, with 80 sccm of O₂ gas flow. Then, the hard mask was removed by submerging the sample in a 5 M nitric acid solution for 20 min. The gel electrolyte was prepared by adding PVA (1g, Poly(vinyl alcohol), Sigma-Aldrich, product number: 341584) in 10 ml of water and stirring the solution overnight at

~50 °C. Once the solution became clear, concentrated H₃PO₄ (0.8 g, Phosphoric acid ≥85%, Sigma-Aldrich, product number: 40278) was added and the solution was stirred overnight at ~50 °C. The gel electrolyte was then deposited on the interdigitated structure and dried overnight. Last, copper contacts were added to the graphene film for electrochemical characterization.

Electrochemical measurements

The CV and GCD measurements were performed with a EG&G Instruments 263A Potentiostat/Galvanostat, Princeton Applied Research. The EIS measurements were performed with a VMP2 potentiostat/galvanostat/frequency response analyzer, BioLogic science instruments. Before the cycling stability test, the device was stabilized for the first 25 cycles. The C_A from CV measurements was extracted with **Equation S1** and the $C_{A,SE}$ from GCD measurements was extracted with **Equation S2**. The capacitance retention during 10000 cycles was calculated by extracting and normalizing the $C_{A,SE}$ from each cycle with Equation S2. The single-electrode volumetric capacitance was extracted with **Equation S3**.

Transmittance measurement

The transmittance spectra were obtained with a UV-vis spectrophotometer (Lambda 750 UV/Vis/NIR spectrophotometer, PerkinElmer). The measurement was performed on the film of graphene flakes (larger than the sample window) before etching. Measuring transmittance before patterning allowed for a more reliable investigation of the transparency of the film, although the final patterned structure is expected to have higher transmittance due to the absence of graphene in the gaps between the fingers. The signal from the glass substrate is treated as the background signal.

Areal and volumetric capacitance extraction

The areal capacitance was calculated with Equation S1:

$$C_A = \frac{1}{A\Delta V} \frac{\int_{0V}^{1V} i dV}{v} \quad (S1)$$

Where A (0.365 cm^2) is the measured geometric area of the interdigitated supercapacitor, i is the response current, v is the scan rate (V/s) and ΔV is the voltage window (V).

The single-electrode areal capacitance was calculated according to Equation S2:

$$C_{A,SE} = 4 \frac{I}{dV/dt A} \quad (S2)$$

Where I is the discharge current, dV/dt is the slope of the linear fit to the discharge curve, A is the geometrical area of the supercapacitor and the factor 4 was used to obtain the single electrode areal capacitance.³

The single-electrode volumetric capacitance was calculated according to Equation S3:

$$C_{V,SE} = 4 \frac{I}{dV/dt V} \quad (S3)$$

Where V refers to the volume of the electrodes.

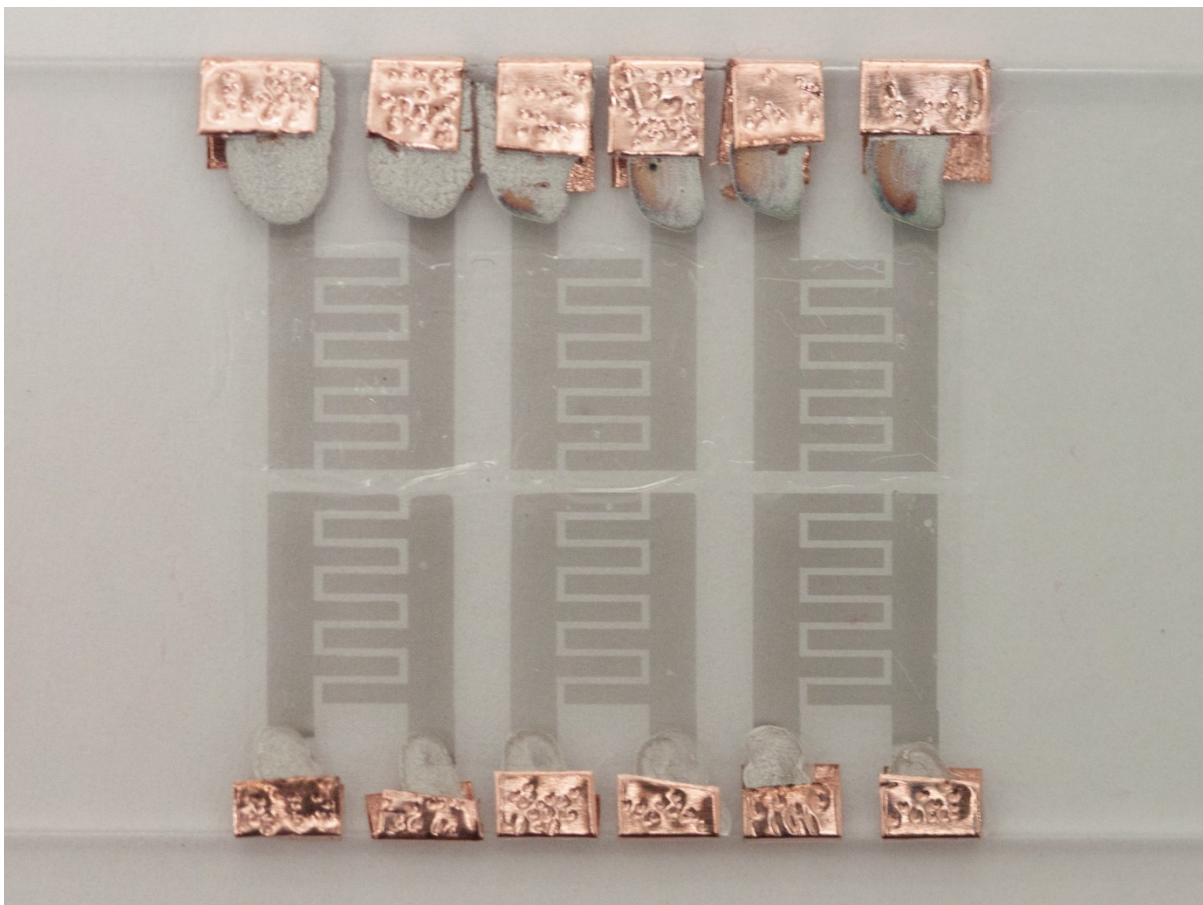


Figure S1. Images of 6 T-MSCs fabricated simultaneously on a glass slide. Gel electrolyte was deposited on the top 3 T-MSCs.

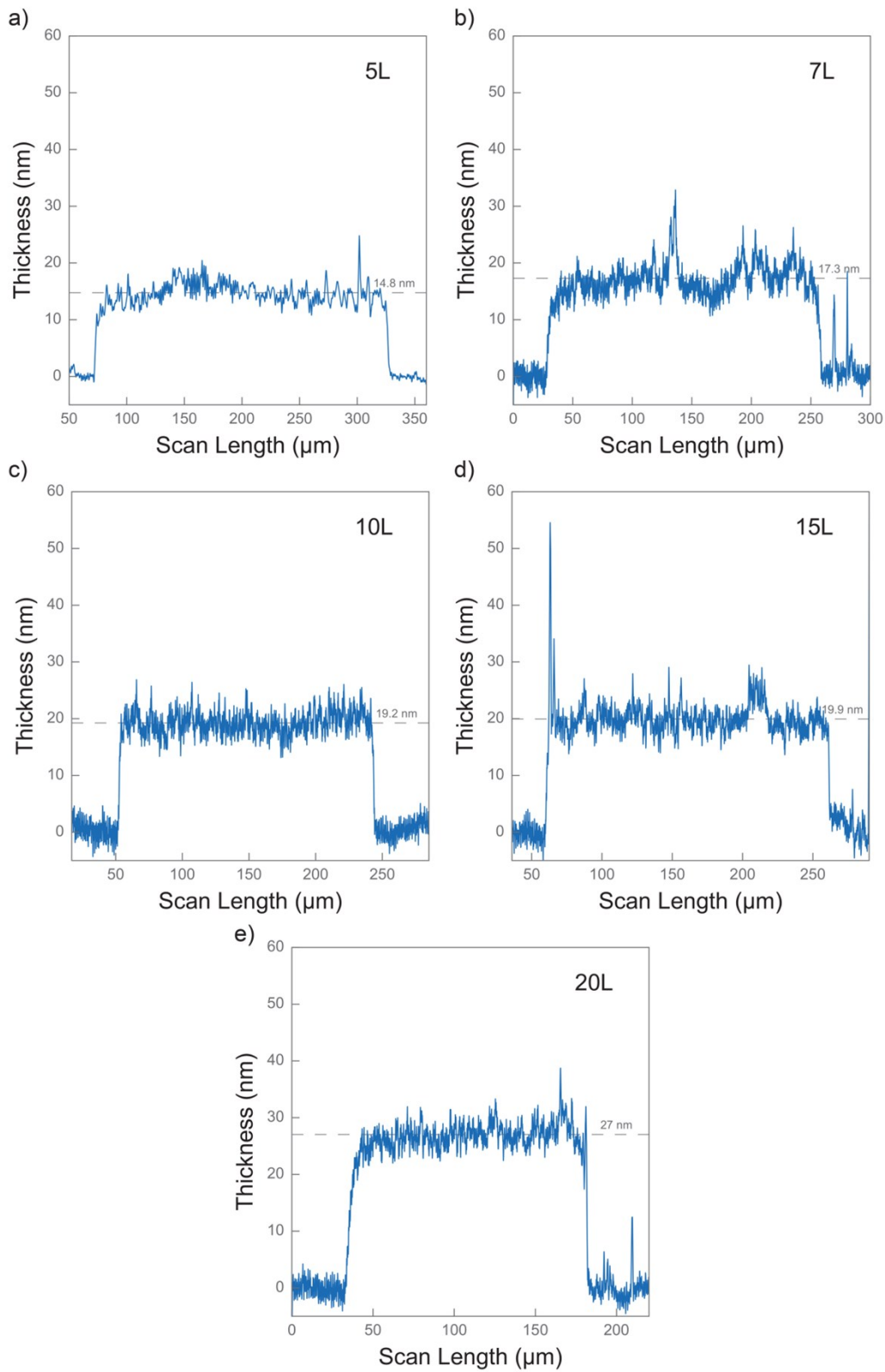


Figure S2. Scan profiles of the graphene electrode of a) 5L, b) 7L, c) 10L, d) 15L and e) 20L devices on a glass substrate. Note that the thickness does not increase linearly with the number of printing passes. The “coffee-ring” effect depletes some solute (graphene) from the inner region thus yielding lower thickness than expected.

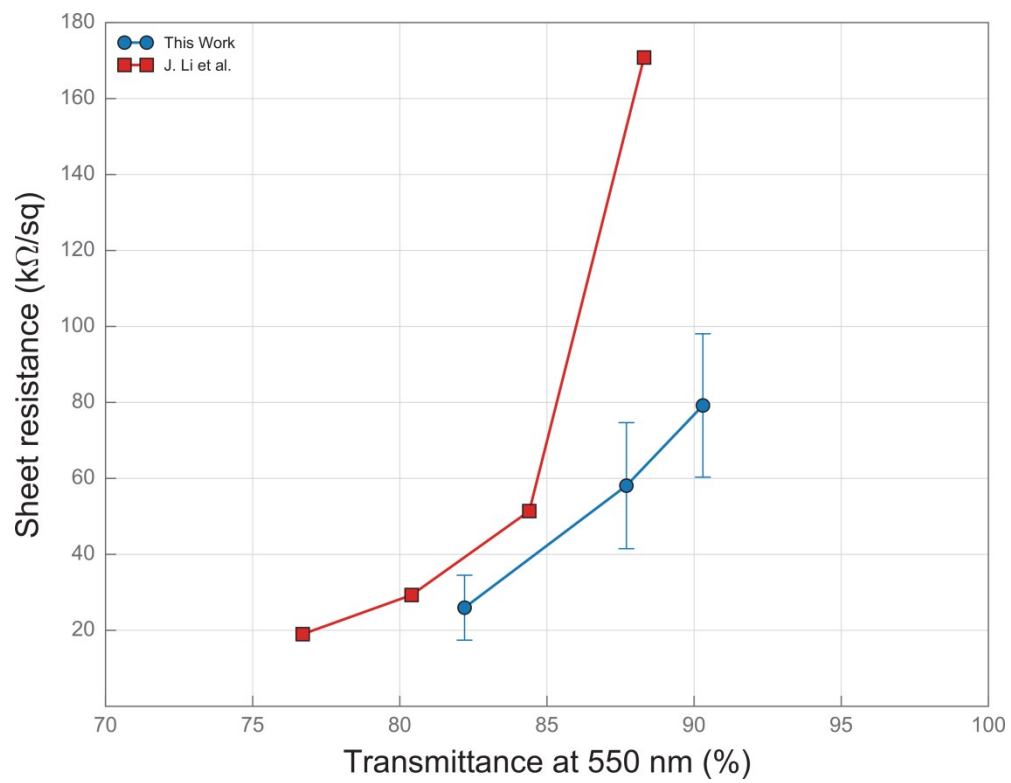


Figure S3. Sheet resistances at different thicknesses (5L, 7L and 10L) and comparison with the previous work of our group.¹ Thanks to the increased uniformity, the sheet resistance is lower at the same transmittance.

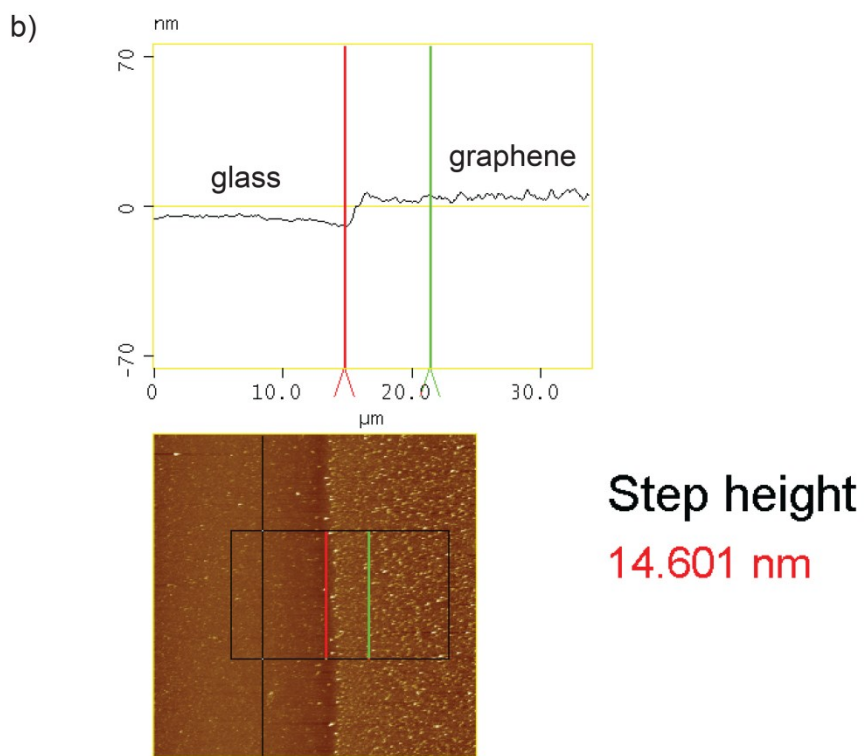
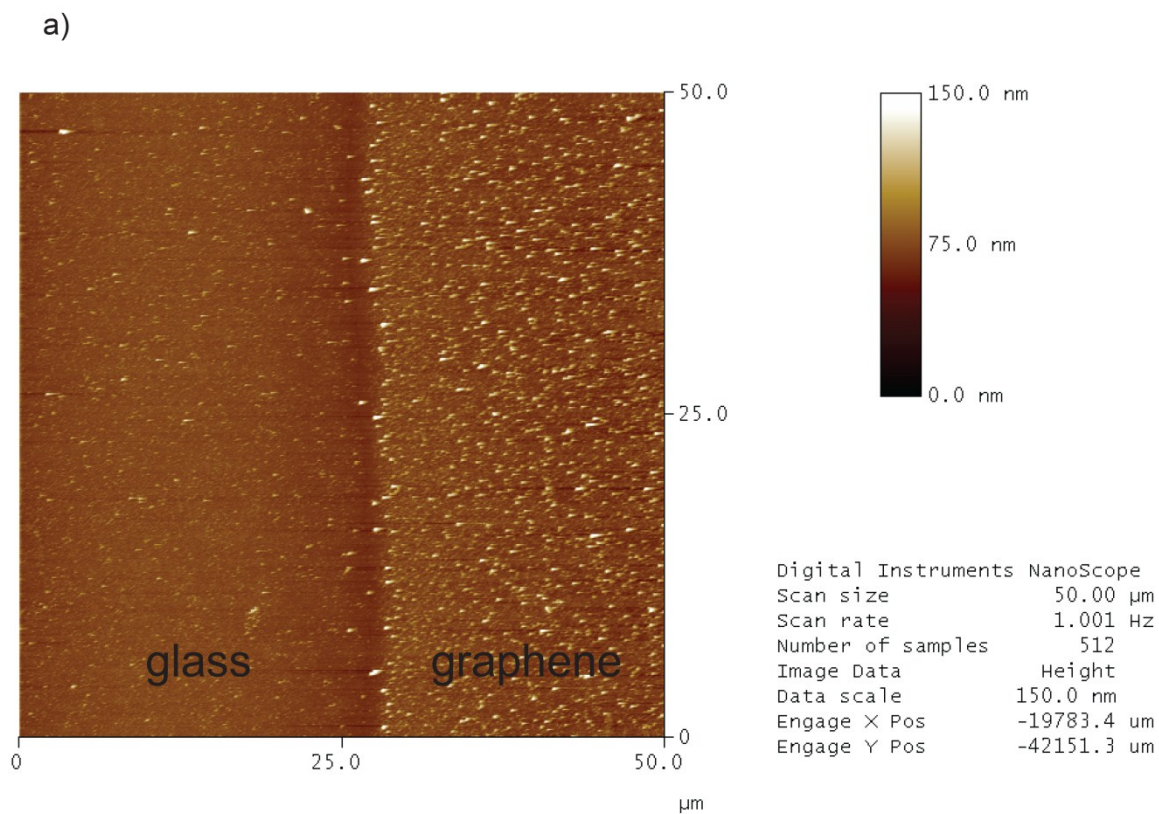


Figure S4. a) AFM image of the pattern boundary of the 5L device. b) Step height extraction from the AFM image.

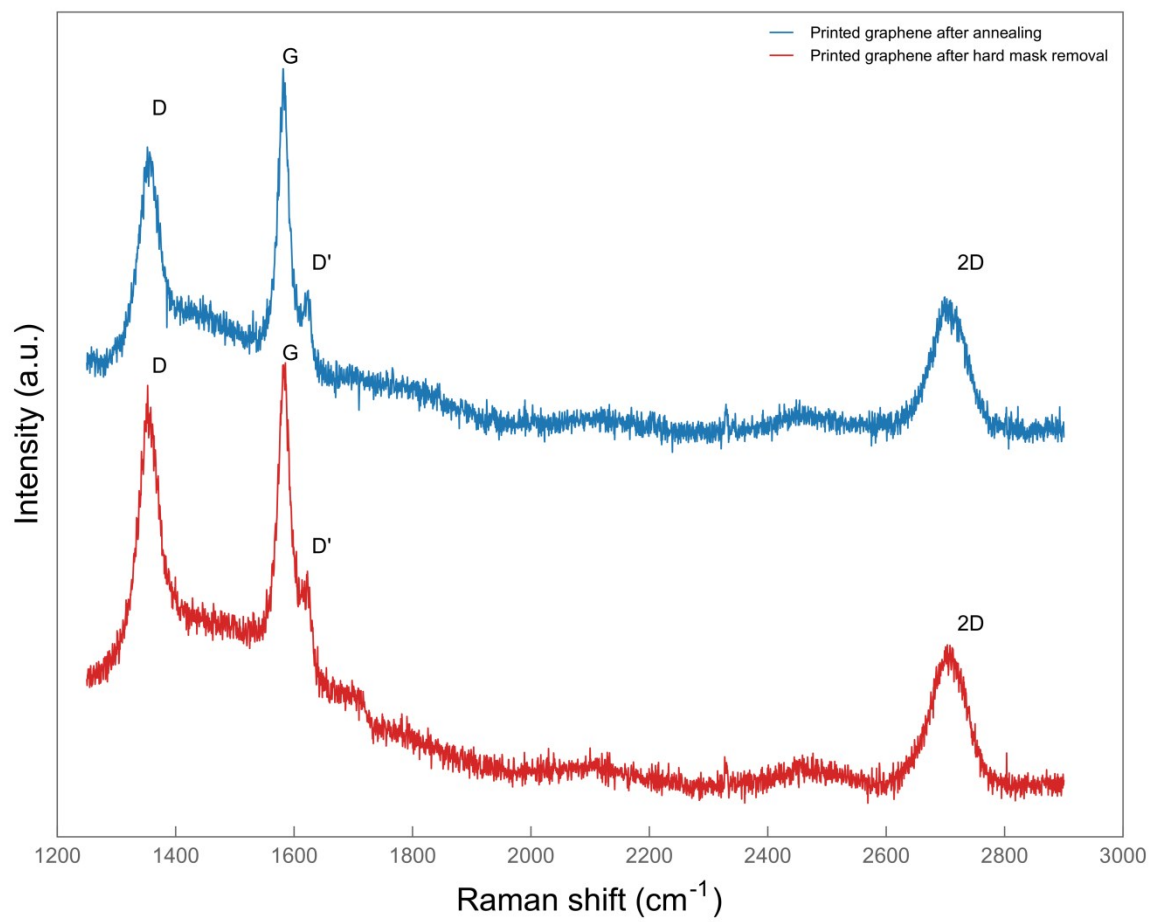


Figure S5. Comparison between Raman spectra of the graphene flakes after annealing (not patterned) and after hard mask removal (O₂ plasma etching + HNO₃ treatment).

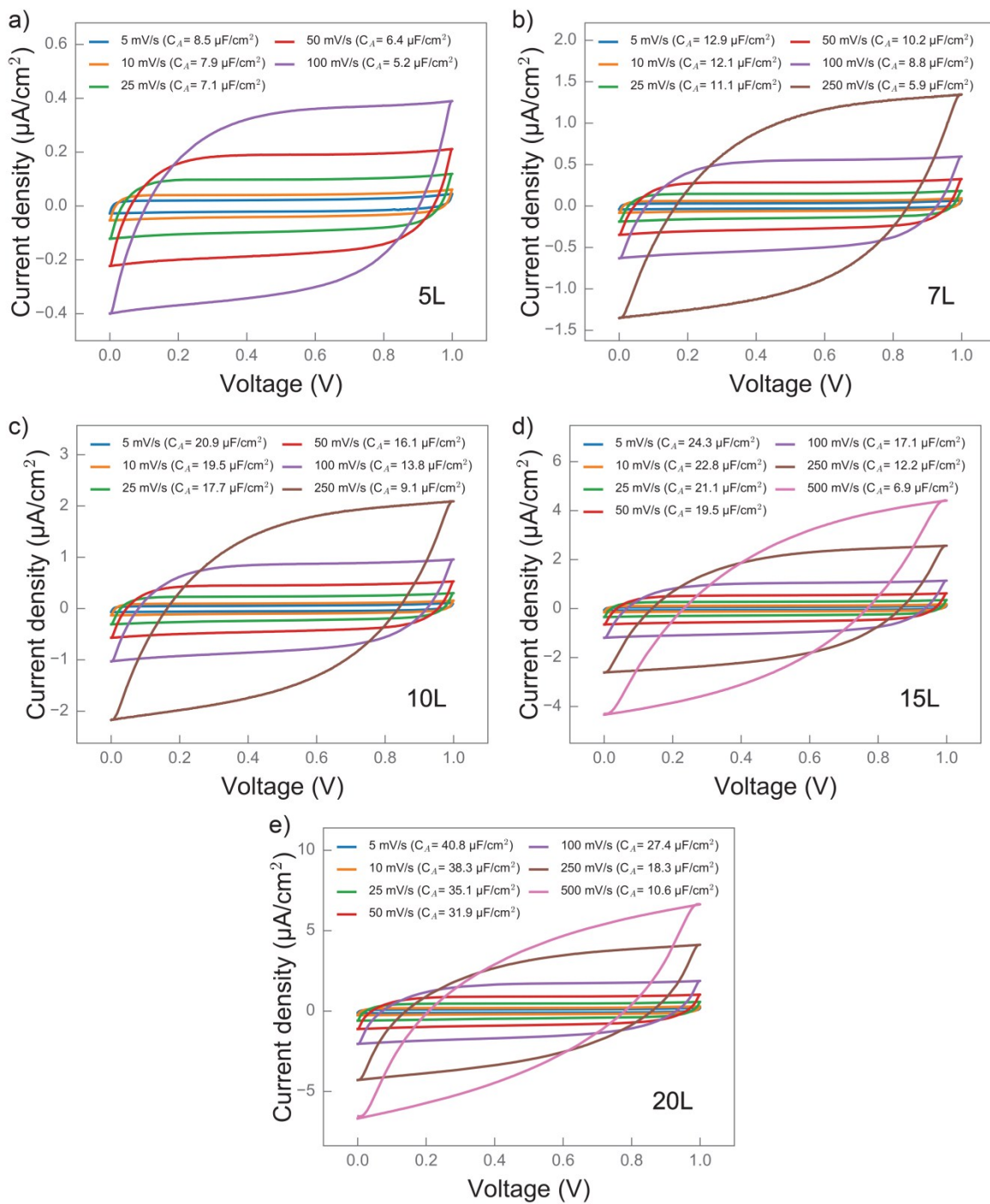


Figure S6. CV curves at different scan rates for the a) 5L, b) 7L, c) 10L, d) 15L and e) 20L devices.

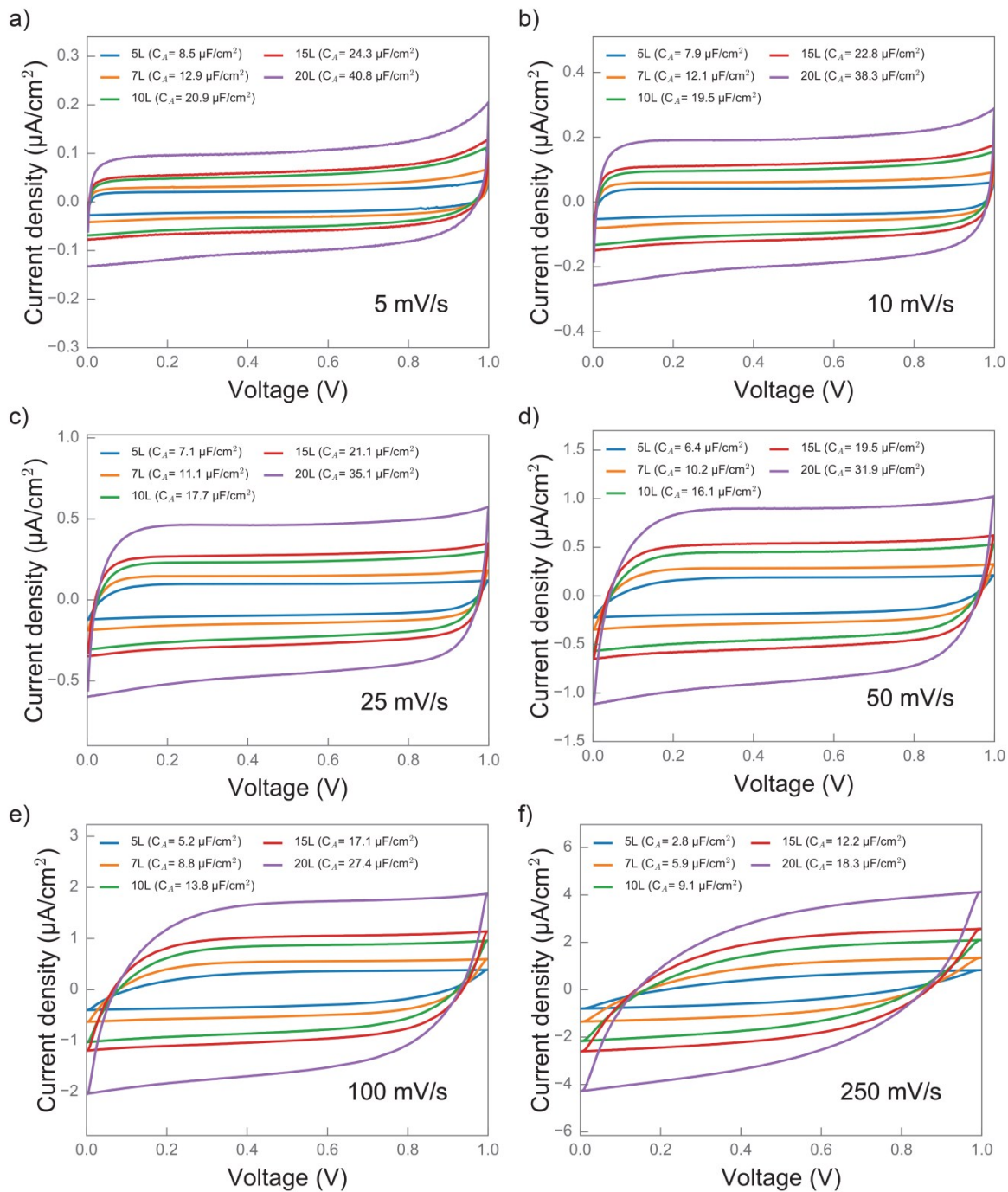


Figure S7. CV curves of devices at different scan rates: a) 5 mV/s, b) 10 mV/s, c) 25 mV/s, d) 50 mV/s, e) 100 mV/s, f) 250 mV/s.

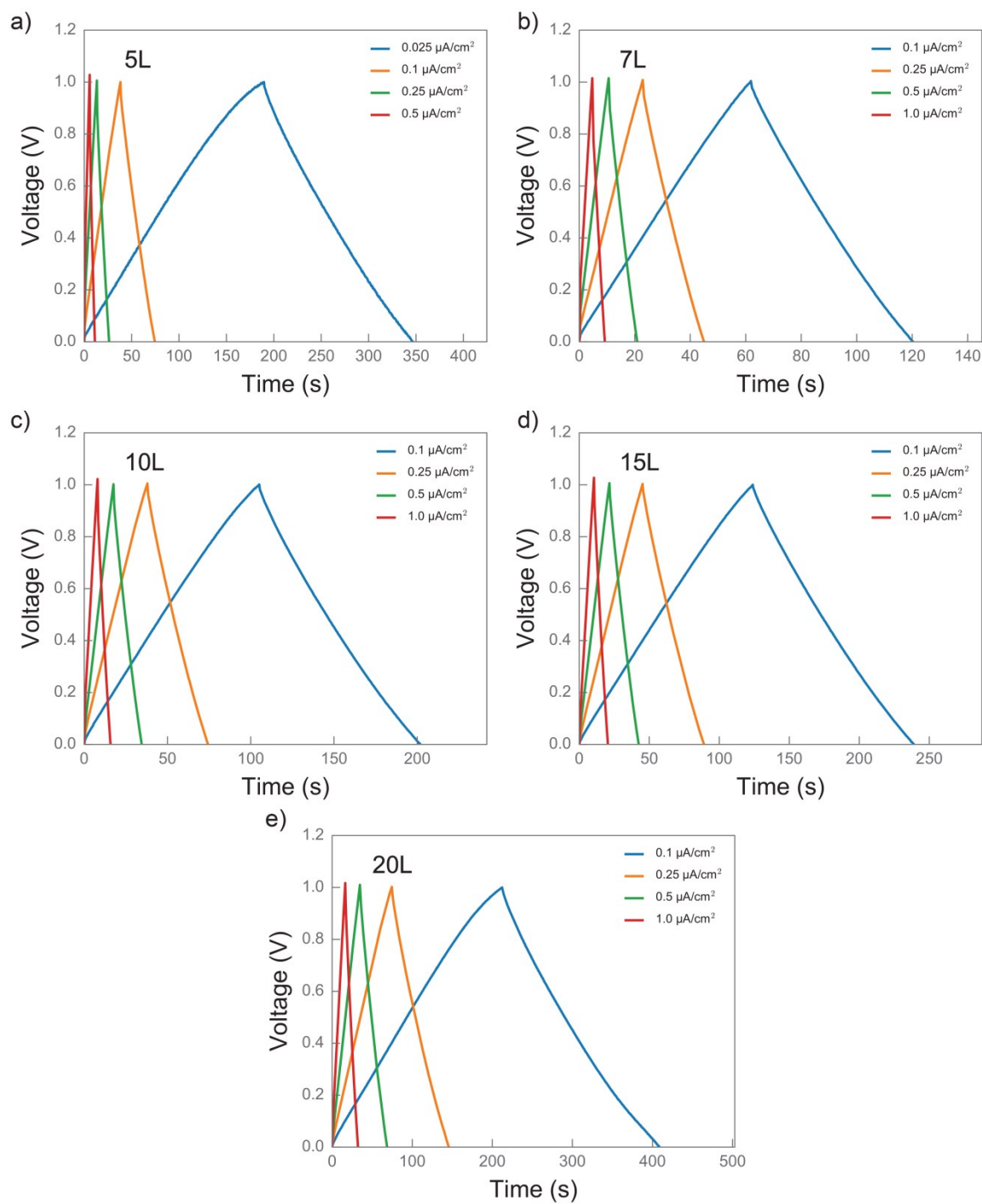


Figure S8. GCD curves at different scan rates of a) 5L, b) 7L, c) 10L, d) 15L and e) 20L devices.

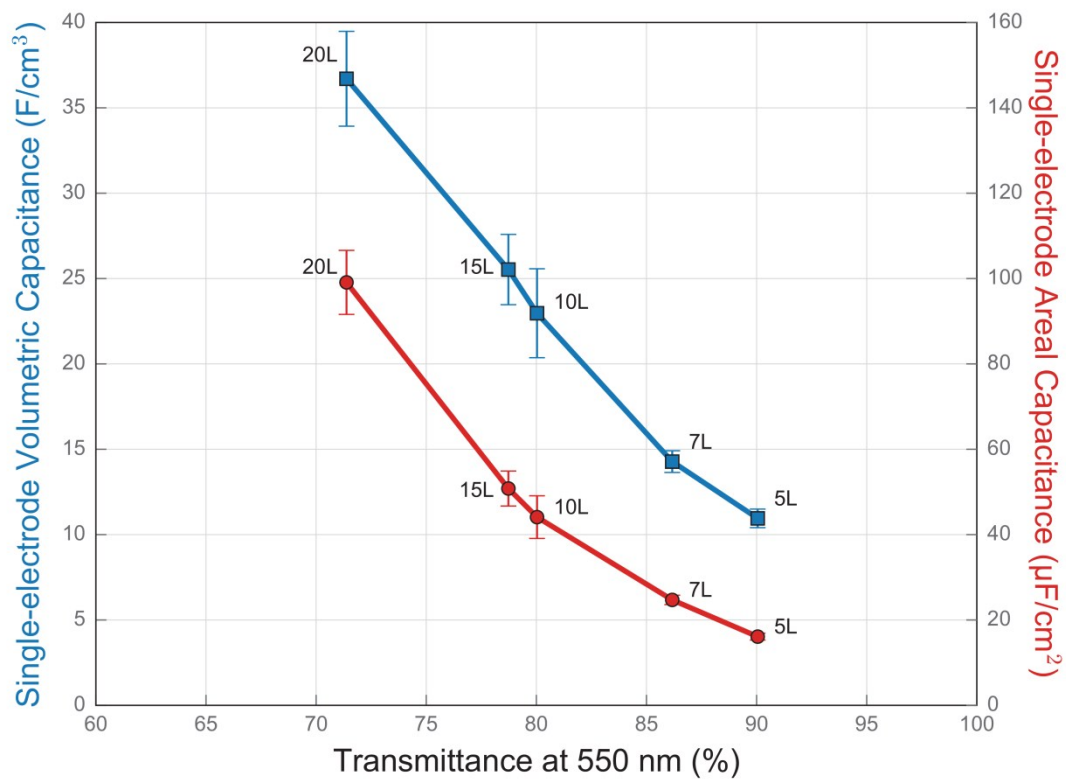


Figure S9. Single-electrode volumetric and areal capacitance of all the devices at different transparencies.

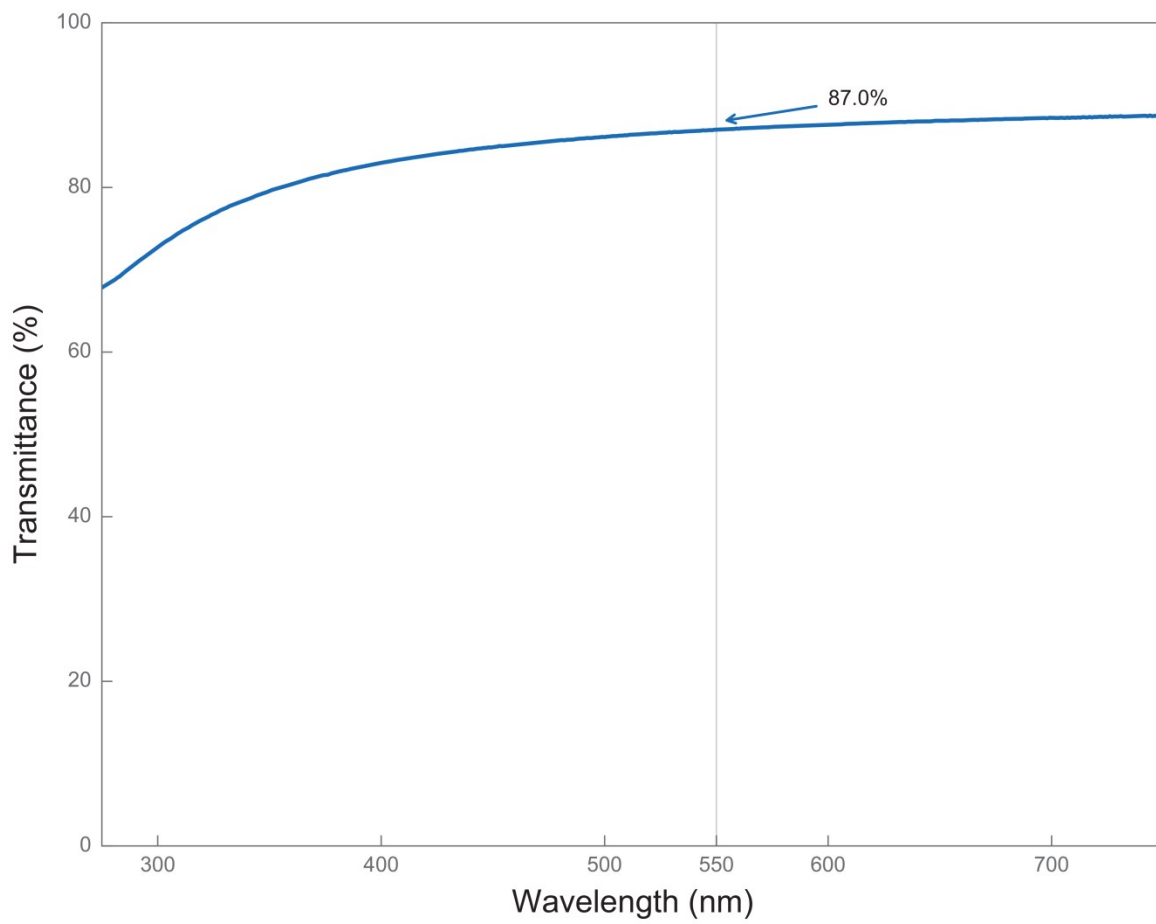


Figure S10. Transmittance spectrum of the 7L device on flexible glass.

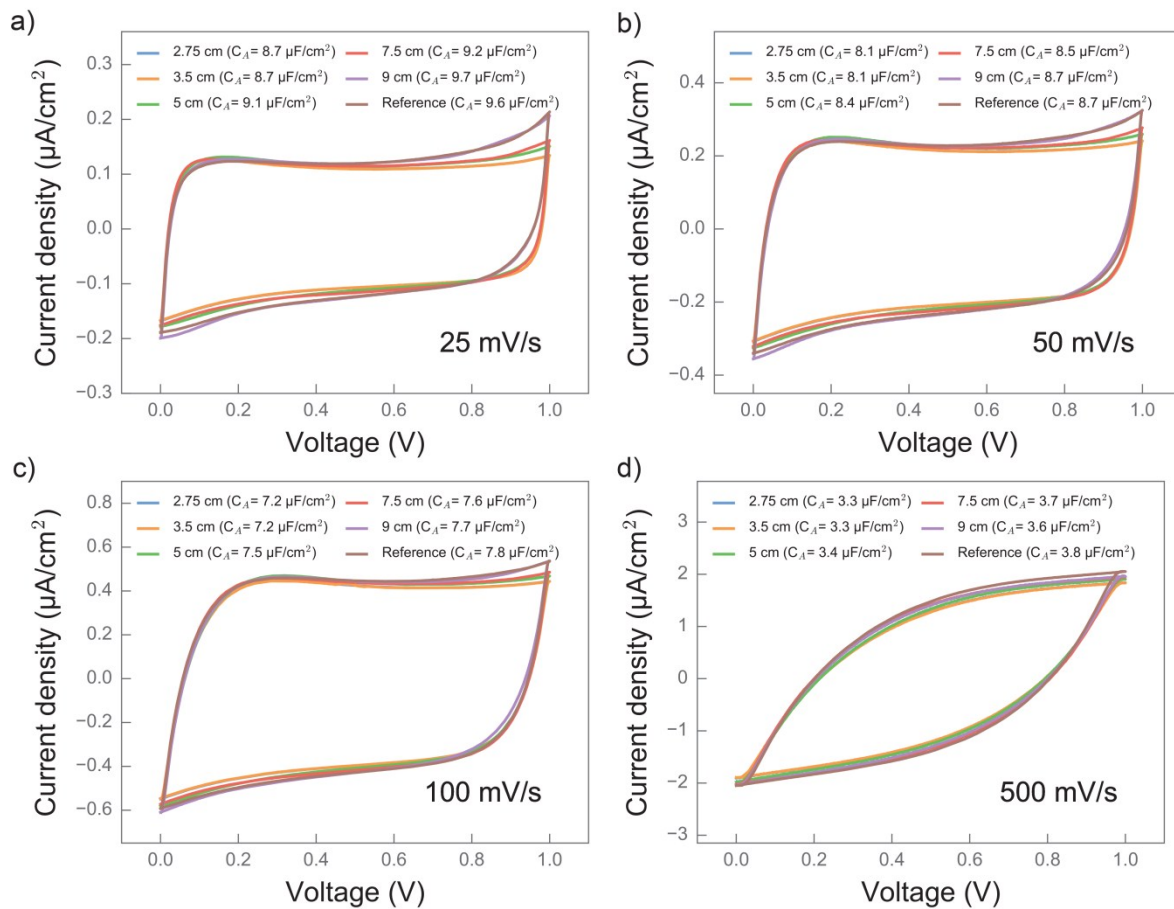


Figure S11. CV curves of the flexible T-MSC under different bending radii at scan rates of: a) 25 mV/s, b) 50 mV/s, c) 100 mV/s and d) 500 mV/s.

Table S1. Comparison of transparent supercapacitors based on graphene in literature. All the devices have PVA/ H₃PO₄ as electrolyte.

| Electrode material | Structure | Technology | C_A ($\mu\text{F}/\text{cm}^2$) (from CV) | $C_{A,SE}$ ($\mu\text{F}/\text{cm}^2$) (from GCD) | Transparency (%) @ 550 nm | Ref. |
|------------------------|-----------|--|--|--|------------------------------|-----------|
| Graphene | Sandwich | RTA | 12.4 (10mV/s) | - | 67 (full device) | 4 |
| Graphene Quantum Dots | Planar | Mask patterning + electrophoretic deposition | - | 9.09 | 92.97 (full device) | 5 |
| Reduced Graphene Oxide | Sandwich | Electrophoretic deposition | - | 1.14 | 75.6 (full device) | 6 |
| CVD graphene | Sandwich | Assembly by pressing | - | 11.6 ^a) | 57 (full device) | 7 |
| Graphene networks | Sandwich | CVD synthesis + assembly | - | 16.8 ^b) | 86 (electrode only) | 8 |
| Graphene flakes | Planar | Inkjet printing + etching | 41.3± 3.7 | 99.1±7.5 | 71.38 (electrodes only) | This work |
| Graphene flakes | Planar | Inkjet printing + etching | 24.3±1.3 | 50.8±4.1 | 78.73 (electrodes only) | This work |
| Graphene flakes | Planar | Inkjet printing + etching | 20.3 ±1.4 | 44.1±5.0 | 80.03 (electrodes only) | This work |
| Graphene flakes | Planar | Inkjet printing + etching | 12.6±0.6 | 24.7±1.1 | 86.17 (electrodes only) | This work |
| Graphene flakes | Planar | Inkjet printing + etching | 8.3±0.3 | 16.1±0.8 | 90.05 (electrodes only) | This work |

^a)We multiplied the reported capacitance by a factor of 2 to obtain $C_{A,SE}$; ^b)We multiplied the reported capacitance by a factor of 4 to obtain $C_{A,SE}$.

References

- 1 J. Li, F. Ye, S. Vaziri, M. Muhammed, M. C. Lemme and M. Östling, *Adv. Mater.*, 2013, **25**, 3985–3992.
- 2 J. Li, M. C. Lemme and M. Östling, *ChemPhysChem*, 2014, **15**, 3427–3434.
- 3 G. Nyström, A. Marais, E. Karabulut, L. Wågberg, Y. Cui and M. M. Hamedi, *Nat. Commun.*, 2015, **6**, 7259.
- 4 Y. Gao, Y. S. Zhou, W. Xiong, L. J. Jiang, M. Mahjouri-Samani, P. Thirugnanam, X. Huang, M. M. Wang, L. J. Jiang and Y. F. Lu, *APL Mater.*, 2013, **1**, 012101.
- 5 K. Lee, H. Lee, Y. Shin, Y. Yoon, D. Kim and H. Lee, *Nano Energy*, 2016, **26**, 746–754.
- 6 M. Wang, L. D. Duong, N. T. Mai, S. Kim, Y. Kim, H. Seo, Y. C. Kim, W. Jang, Y. Lee, J. Suhr and J.-D. Nam, *ACS Appl. Mater. Interfaces*, 2015, **7**, 1348–1354.
- 7 T. Chen, Y. Xue, A. K. Roy and L. Dai, *ACS Nano*, 2014, **8**, 1039–1046.
- 8 X. Fan, T. Chen and L. Dai, *RSC Adv.*, 2014, **4**, 36996–37002.